

Development of Targetable Two-Photon Fluorescent Probes to Image Hypochlorous Acid in Mitochondria and Lysosome in Live Cell and Inflamed Mouse Model

Lin Yuan,^{†,‡,||} Lu Wang,^{†,||} Bikram Keshari Agrawalla,[†] Sung-Jin Park,[§] Hai Zhu,[†] Balasubramaniam Sivaraman,[§] Juanjuan Peng,[§] Qing-Hua Xu,[†] and Young-Tae Chang^{*,†,§}

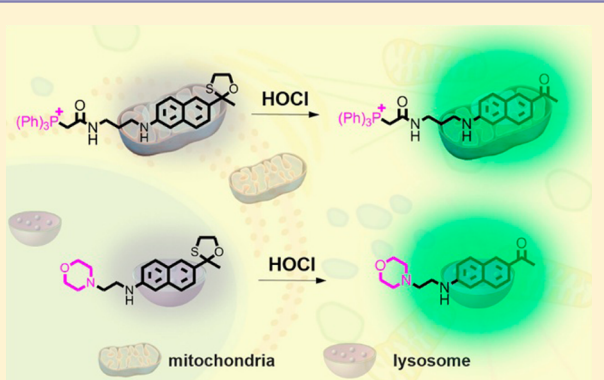
[†]Department of Chemistry, National University of Singapore, Singapore 117543

[‡]State Key Laboratory of Chemo/Biosensing and Chemometrics, College of Chemistry and Chemical Engineering, Hunan University, Changsha 410082, PR China

[§]Laboratory of Bioimaging Probe Development, Singapore Bioimaging Consortium, Singapore 117543

Supporting Information

ABSTRACT: Hypochlorous acid (HOCl), as a highly potent oxidant, is well-known as a key “killer” for pathogens in the innate immune system. Recently, mounting evidence indicates that intracellular HOCl plays additional important roles in regulating inflammation and cellular apoptosis. However, the organelle(s) involved in the distribution of HOCl remain unknown, causing difficulty to fully exploit its biological functions in cellular signaling pathways and various diseases. One of the main reasons lies in the lack of effective chemical tools to directly detect HOCl at subcellular levels due to low concentration, strong oxidization, and short lifetime of HOCl. Herein, the first two-photon fluorescent HOCl probe (TP-HOCl 1) and its mitochondria- (MITO-TP) and lysosome- (LYSO-TP) targetable derivatives for imaging mitochondrial and lysosomal HOCl were reported. These probes exhibit fast response (within seconds), good selectivity, and high sensitivity (<20 nM) toward HOCl. In live cell experiments, both probes MITO-TP and LYSO-TP were successfully applied to detect intracellular HOCl in corresponding organelles. In particular, the two-photon imaging of MITO-TP and LYSO-TP in murine model shows that higher amount of HOCl can be detected in both lysosome and mitochondria of macrophage cells during inflammation condition. Thus, these probes could not only help clarify the distribution of subcellular HOCl, but also serve as excellent tools to exploit and elucidate functions of HOCl at subcellular levels.



INTRODUCTION

The study of reactive oxygen species (ROS) is attracting increasing attention due to their essential roles in cell signaling and homeostasis, such as aging,¹ pathogen response,² and anti-inflammation regulation.³ Among various ROS, hypochlorous acid (HOCl) as a highly potent oxidant generated during phagocytosis seems to mainly serve as a “killer” for pathogens in the innate immune system.⁴ It is usually produced by myeloperoxidase (MPO)-catalyzed per-oxidation of chloride ions in phagolysosome, where pathogens are engulfed and decomposed⁵ (Figure 1). In addition to phagosomal HOCl in the presence of pathogens, mounting evidence demonstrates that nonphagosomal intracellular HOCl (nphHOCl) generation can be induced by a variety of soluble stimuli,^{6,7} which helps suppress inflammation and regulate cellular apoptosis.^{8,9} Furthermore, it is reported that nphHOCl may also be implicated in neurodegenerative disorders¹⁰ such as Parkinson’s disease¹¹ and cerebral ischemia.¹² At the same time, HOCl could cause mitochondrial permeabilization,¹³ lysosomal rupture,¹⁴ and cell death through calcium dependent calpain

activation.¹³ However, the distribution of nphHOCl at subcellular levels is still unclear, which causes severe difficulty to fully exploit and elucidate intracellular functions of nphHOCl.¹⁵ One of the main reasons lies in lack of efficient tools to directly real-time monitor nphHOCl at the subcellular level due to its strong oxidization,¹⁶ short-lived time,¹⁷ and relatively low concentration.¹⁸ Therefore, it is challenging and highly desired to prepare novel chemical tools for elucidating the distribution and functions of nphHOCl at subcellular level.

Fluorescence imaging possesses unique advantages for the observation of functional and molecular recognition events in live cells.^{19,20} Furthermore, it has emerged as the irreplaceable technique to monitor the level, localization, and movement of biomolecules at subcellular levels.^{21–25} Among various types of optical imaging techniques, two-photon microscopy (TPM) offers high-resolution imaging, deep penetration, and low phototoxicity due to the remarkably focused excitation and

Received: January 3, 2015

Published: April 23, 2015

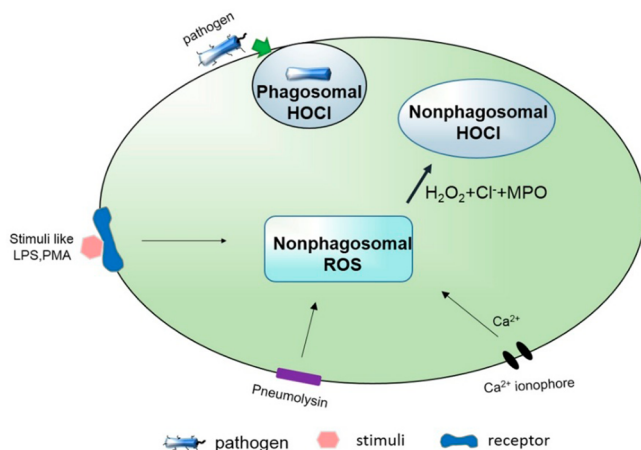


Figure 1. Stimuli that induce intracellular HOCl. Apart from ingested particles that give rise to phagosomal HOCl (phHOCl) production (left), certain stimuli, such as lipopolysaccharides (LPS), lead to nonphagosomal HOCl (nphROS) production without being ingested (right). H_2O_2 , hydrogen peroxide; MPO, myeloperoxidase.

reduced scattering of near-infrared light in biological tissues.^{26–29} Recently, the detection of HOCl was implemented by some good probes with different recognition moieties, including dibenzoylhydrazine,³⁰ *p*-methoxyphenol,^{31,32} oxime^{33–36} selenide,^{37–40} thiol compounds (internal thioester,^{41–44} thioether,^{45,46,6,72} and thiosemicarbazide⁴⁸), and other groups,^{47,49,64} which are specified in Supporting Information Table S1. Even though most of these probes have been successfully applied to image intracellular HOCl, few probes were used to real-time detect HOCl at subcellular levels. On the other hand, it was assumed that nphHOCl may be

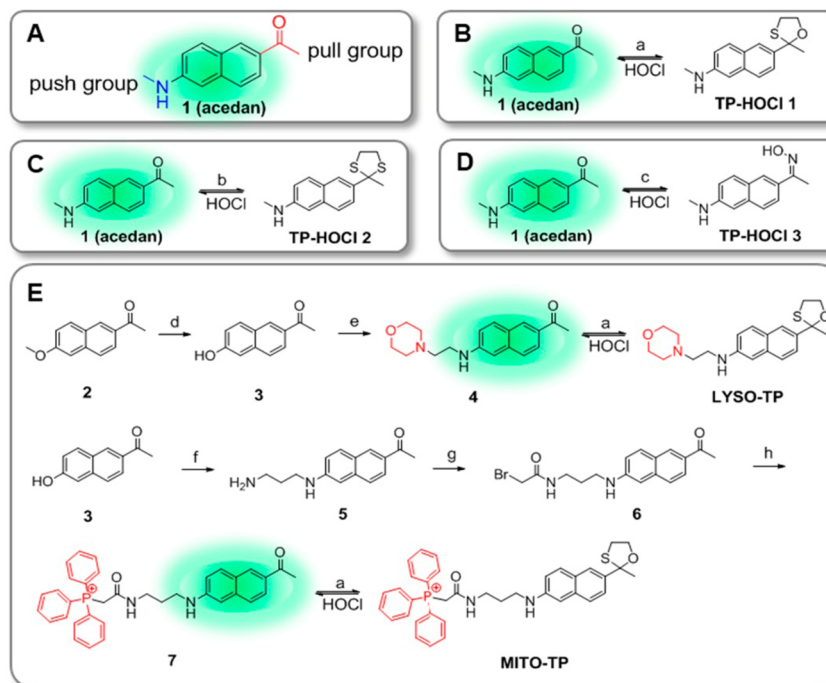
generated in both mitochondria and lysosome of macrophage cells due to the intracellular distribution of MPO that catalyzes HOCl production.^{50,51} Nevertheless, to the best of our knowledge, except for several mitochondria-located fluorescent probes for the detection of intracellular HOCl,^{46,52,73} there is no report yet describing a fluorescent probe for successful detection of intracellular HOCl in lysosome, even though there were two reported lysosome targeting probes with exogenously added HOCl.^{40,53} The aforementioned concerns encouraged us to develop novel two-photon fluorescent probes to sense this important biomolecule and clarify its distribution in live cell and inflamed mouse model.

Herein, we report the first two-photon fluorescent “turn-on” HOCl probe (TP-HOCl 1) and its mitochondria- (MITO-TP) and lysosome- (LYSO-TP) targetable derivatives, which can image intracellular HOCl in live cell and inflamed mouse model. In the presence of HOCl, TP-HOCl 1 exhibits a dramatic fluorescence increase with very short response time (within seconds), excellent selectivity, and high sensitivity (16.6 nM). Besides, in live cell experiments, it is clearly indicated that MITO-TP and LYSO-TP can respond toward HOCl in mitochondria and lysosome. Furthermore, these probes were successfully applied to image mitochondrial and lysosomal HOCl in inflamed mouse model through two-photon imaging.

RESULTS AND DISCUSSION

Design and Synthesis of HOCl Probes. Acedan, as a well-known two-photon fluorophore,^{54–57} was chosen as the fluorescence reporting group due to its excellent photophysical properties resulting from the typical “push–pull” (amine-ketone) structure (Scheme 1A).⁵⁷ Thus, it is predictable that protection of the ketone will decrease the “pull” ability thereby

Scheme 1. Synthesis and Proposed Sensing Mechanism of Probes for HOCl^a



^aReagents and conditions: (a) 2-mercaptopropanoic acid, 50 °C, 3 h; (b) 1,2-ethanedithiol, 50 °C, 3 h; (c) hydroxylamine, 50 °C, 3 h; (d) 37% HCl, reflux, 48 h; (e) 2-morpholinoethanamine, Na₂S₂O₈, microwave 80 W, 160 °C, 5 h; (f) propane-1,3-diamine, Na₂S₂O₈, microwave 80 W, 160 °C, 6 h; (g) 2-bromoacetyl chloride, rt, 50 min; (h) triphenylphosphine, rt, 16 h.

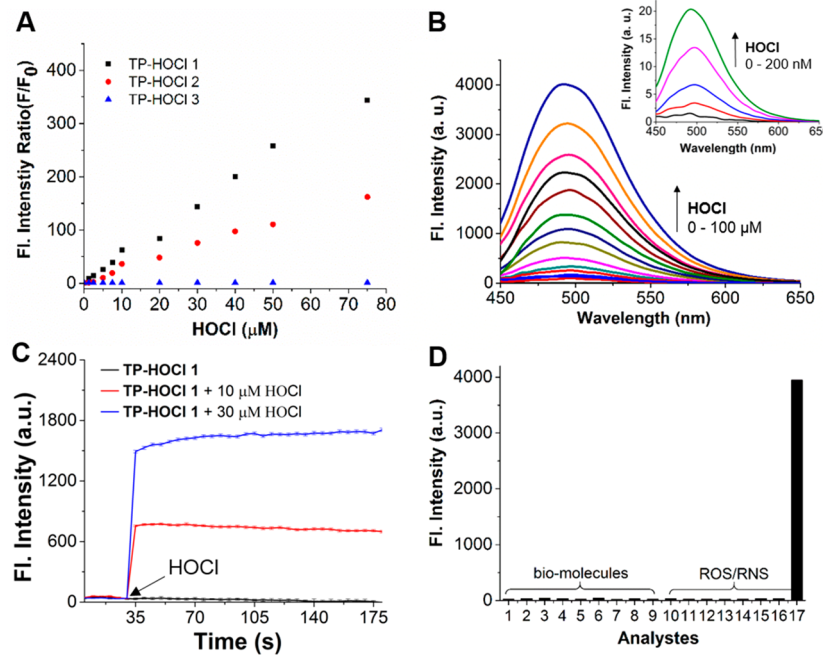


Figure 2. Fluorescence spectra of TP-HOCl 1–3 responding to HOCl in PBS/EtOH (1:1, pH 7.4) solution. (A) Plot of fluorescence intensity ratio (F/F_0 at 500 nm) changes of TP-HOCl 1–3 as a function of HOCl concentrations; data acquired at 20 s after addition of HOCl ($\lambda_{\text{ex}} = 375 \text{ nm}$). (B) Fluorescence enhancement of TP-HOCl 1 (5 μM) as a function of HOCl (0 to 100 μM). Inset shows Fluorescence spectra of TP-HOCl 1 (0.5 μM) before and after adding HOCl at low concentrations (0–200 nM). (C) Time course of fluorescence intensity of TP-HOCl 1 before and after adding 10 and 30 μM HOCl. (D) Fluorescence responses of TP-HOCl 1 (5 μM) toward various analytes (50 μM for biomolecules (1–9) and 100 μM for other ROS/RNS (10–17)). (1) PBS; (2) ATP; (3) ADP; (4) NAD; (5) GSH; (6) Cys; (7) Fe^{3+} ; (8) Zn^{2+} ; (9) Cu^{2+} ; (10) H_2O_2 ; (11) $\bullet\text{OH}$; (12) $t\text{-BuOOH}$; (13) $t\text{-BuOO}^\bullet$; (14) NO^\bullet ; (15) O_2^- ; (16) ONOO^- ; (17) HOCl.

quenching the fluorescence of acedan. On the other hand, it is reported that the thiol atom in methionine is easily oxidized in tandem to sulfoxide and sulfone by HOCl.⁵⁸ Thus, 2-mercaptoproethanol and 1, 2-ethanedithiol were employed to protect the ketone of acedan in the design of HOCl probes (TP-HOCl 1 and TP-HOCl 2). It was expected that both compounds will be nonfluorescent or weakly fluorescent due to the disruption of the “push–pull” structure; however, reaction with HOCl, which deprotects the oxathiolane/mercaptal group to reveal the ketone, would lead to fluorescence enhancement. This expectation was further supported by the significantly increased oscillator strength of TP-HOCl 1 (f , from 0.067 to 0.44) before and after reacting with HOCl calculated by density functional theory (DFT) (Figure S1). For comparison, oxime, a known reaction site for HOCl,^{33,34,36,59} was also introduced by combining hydroxylamine with acedan (TP-HOCl 3). Through comparison of response ability of three probes to HOCl, TP-HOCl 1 was chosen as the ideal HOCl probe, which is specified in the following paragraphs.

To monitor HOCl at subcellular levels, lysosome- and mitochondria-targetable groups (morpholine⁶⁰ and triphenylphosphine⁶¹) were further introduced to ensure the probe’s intracellular localization. In addition, to avoid affecting the sensitivity of the probe, these groups were carefully positioned at the other end of acedan to generate long distance gap from the reaction site. The lysosomal HOCl probe LYSO-TP and mitochondrial HOCl probe MITO-TP were effectively prepared from cyclization reaction of precursor 4 or 7 with 2-mercaptoproethanol (Scheme 1E). The precursor 4 was synthesized through the hydrolysis of commercially available dye 6-methoxy-2-acetonaphthone and subsequent amination of intermediate 3 with 4-(2-aminoethyl)morpholine. The pre-

cursor 7 was readily synthesized through amination of intermediate 3 with 1,3-propanediamine, and then amide coupling with 2-bromoacetyl chloride, and finally salt formation with triphenylphosphine. The detailed synthetic procedures, NMR and HRMS spectra are displayed in the Supporting Information.

Comparing the Fluorescent Response of TP-HOCl 1–3 to HOCl. To compare the fluorescent response of TP-HOCl 1–3 to HOCl, three probes were titrated with HOCl from 0 to 75 μM . Compared to TP-HOCl 2, the fluorescence intensity ratio (F/F_0 at 500 nm) of TP-HOCl 1 was enhanced more significantly at low concentration of HOCl (Figure 2A), thereby indicating higher sensitivity. One reason may be due to the single sulfur atom in 1,3-oxathiolane, which would require less HOCl for complete oxidation of TP-HOCl 1. Different from the case of TP-HOCl 1 and TP-HOCl 2, oxime-based probe TP-HOCl 3 shows only slight response to HOCl, which may be attributed to the more effective oxidative deprotection of oxime by HOCl under basic conditions.³³ Therefore, TP-HOCl 1 was chosen as the probe for HOCl detection and its basic photophysical properties were examined (Table S2 and Figure S2).

Fluorescent response of TP-HOCl 1 to HOCl. To investigate the sensitivity, selectivity and response time of TP-HOCl 1 to HOCl, fluorescence spectroscopy was measured at various concentrations of HOCl. As it is shown in Figure 2B, the fluorescence intensity of TP-HOCl 1 at 500 nm increased more than 670-fold when 20 equiv of HOCl was added, which results from the recovery of “push–pull” structure of acedan when the oxathiolane was deprotected by HOCl. Moreover, TP-HOCl 1 could respond to low concentration of HOCl with detection limit up to 16.6 nM (Figure S3), which indicates the

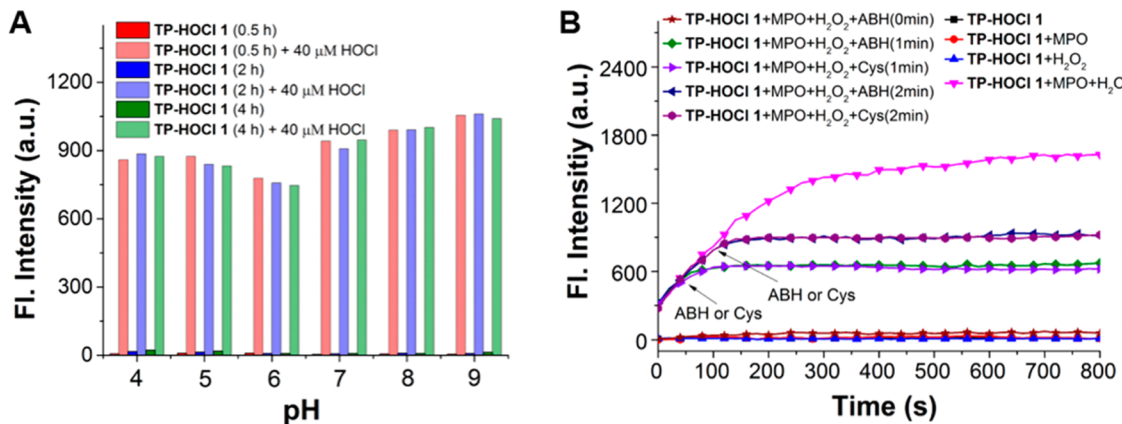


Figure 3. (A) Probe TP-HOCl 1 ($5\ \mu\text{M}$) could kept stable in physiological pHs (pH 4–8). Probe was incubated in various pH buffers (pH 4–9) for 0.5, 2, and 4 h, and then $40\ \mu\text{M}$ HOCl was added. (B) Fluorescence responses of TP-HOCl 1 toward HOCl generated in MPO/ $\text{H}_2\text{O}_2/\text{Cl}^-$ system (PBS, $20\ \mu\text{M}$ H_2O_2 , 1 U/mL MPO, pH = 7.4, 37°C). ABH (4-aminobenzoic acid hydrazide, $10\ \mu\text{M}$) or Cys (cysteine, $200\ \mu\text{M}$) was added at 1 and 2 min, respectively. MPO, myeloperoxidase; ABH, MPO inhibitor.

high sensitivity of probe TP-HOCl 1 to HOCl and the ability of probe TP-HOCl 1 to monitor trace amounts of intracellular HOCl. In addition, the time dependent fluorescence intensity changes of probe TP-HOCl 1 to HOCl revealed that the reaction can be completed within seconds at different pH buffer (pH 5.5, 7.4, 9.2) and the fluorescent signals remained nearly unchanged over time (Figures 2C and S4), which enables its real-time detection of HOCl. However, no fluorescence change was observed when TP-HOCl 1 was incubated with other ROS ($50\ \mu\text{M}$) and biomolecules ($100\ \mu\text{M}$) (Figure 2D). In addition, selectivity (HOCl $50\ \mu\text{M}$ and other ROS $250\ \mu\text{M}$) was further examined at pH 5.5 and 7.8, which were chosen to mimic the lysosomal and mitochondrial pH, respectively. As shown in Figure S5, TP-HOCl 1 can also respond to HOCl rather than other ROS in both weak acid and basic environment. Notably, H_2O_2 , a precursor of HOCl, does not interfere with the detection of HOCl even at $500\ \mu\text{M}$ (Figure S6). In addition, TP-HOCl 1 displayed almost no response to another highly potent oxidant, peroxynitrite (ONOO^-) (Figure S7), in good agreement with previous reported probes with thioester^{41–44} and thioether^{45,46,6,39} as recognition moieties. TP-HOCl 1 is thus a good HOCl probe with high sensitivity, remarkable selectivity and very short response time.

Effect of pH to Response Ability and Stability of TP-HOCl 1. To test the feasibility of TP-HOCl 1 as HOCl probe, the performance of TP-HOCl 1 to HOCl in PBS buffers with different pH values ranging from 4 to 9 was tested. As shown in Figure S8, after addition of HOCl, remarkable fluorescence enhancement of TP-HOCl 1 could be observed immediately at wide pH ranges (pH 4–9) without significant variances, indicating that the assay is compatible with most intracellular pH environments. Even though it was reported that pH may affect the oxidizing rate of hypochlorite,⁶² it was difficult to discriminate the difference under various pH conditions because of the fast response of thioether to hypochlorite, which can be achieved within seconds. Similar results can also be observed in the previous thioether-based probes.^{45,63} Meanwhile, a stability test for TP-HOCl 1 in PBS buffer was also conducted to check whether the oxathiolane group of TP-HOCl 1 is stable at intracellular pH values (pH 4–9). As indicated by Figure 3A, almost no fluorescence changes were observed even after 4 h incubation, while strong fluorescence was recovered after addition of $40\ \mu\text{M}$ HOCl, which suggests

the stability of TP-HOCl 1. Therefore, these results clearly demonstrate the feasibility of TP-HOCl 1 responding toward HOCl in a broad range of pHs.

Fluorescent Response of TP-HOCl 1 to HOCl Generated in Myeloperoxidase (MPO)/ $\text{H}_2\text{O}_2/\text{Cl}^-$ System. With the favorable features of TP-HOCl 1 demonstrated, the feasibility of real-time detection of HOCl generation in an enzyme system was further investigated. MPO/ $\text{H}_2\text{O}_2/\text{Cl}^-$ system (PBS, $20\ \mu\text{M}$ H_2O_2 , 1 U/mL MPO, pH = 7.4, 37°C) was used to mimic the generation of HOCl inside cells. As shown in Figure 3B, the fluorescence intensity of TP-HOCl 1 was increased immediately after addition into MPO/ $\text{H}_2\text{O}_2/\text{Cl}^-$ system. Continuous fluorescence increase over time was observed (within 15 min) due to gradual production of HOCl. Nevertheless, almost no variation in the fluorescent signals was observed in the presence of only MPO or H_2O_2 , which demonstrated that HOCl rather than H_2O_2 or MPO is the target analyte. Furthermore, there is no obvious signal increase after inhibition of MPO by addition of 4-aminobenzoic acid (ABH, an MPO inhibitor) into the MPO/ $\text{H}_2\text{O}_2/\text{Cl}^-$ system. Importantly, after addition of ABH or cysteine at 1 and 2 min, the increasing fluorescence intensity was inhibited immediately thereby showing plane lines. Taken all together, TP-HOCl 1 was successfully used in real-time detection of HOCl generation in MPO/ $\text{H}_2\text{O}_2/\text{Cl}^-$ system, enabling itself to be a promising probe for studying HOCl-related biological processes.

Mechanism of TP-HOCl 1 Responding to HOCl. To further examine the sensing mechanism of probe TP-HOCl 1, reversed-phased HPLC-MS was used to clarify the process of the reaction between TP-HOCl 1 and HOCl. The HPLC chromatograms of TP-HOCl 1 and compound 1 are shown in Figure S9A and D. After incubation with HOCl ($100\ \mu\text{M}$ and $200\ \mu\text{M}$) for 1 min (Figure S9C, D), except for the peaks from TP-HOCl 1 and deprotected compound 1, a new peak with longer retention time was observed. This compound was purified and identified as the chlorinated product (compound 9) through ^1H NMR, ^{13}C NMR and, HRMS (Figure S10A–C). Meanwhile, the position of chlorine atom was further verified by H–H COSY, indicating that chlorine atom locates at C-7 rather than C-5 (Figure S10D). A similar chlorination reaction with HOCl was also observed in other fluorophores, such as Si-fluorescein and rhodamine.^{43,64} In particular, the photo-

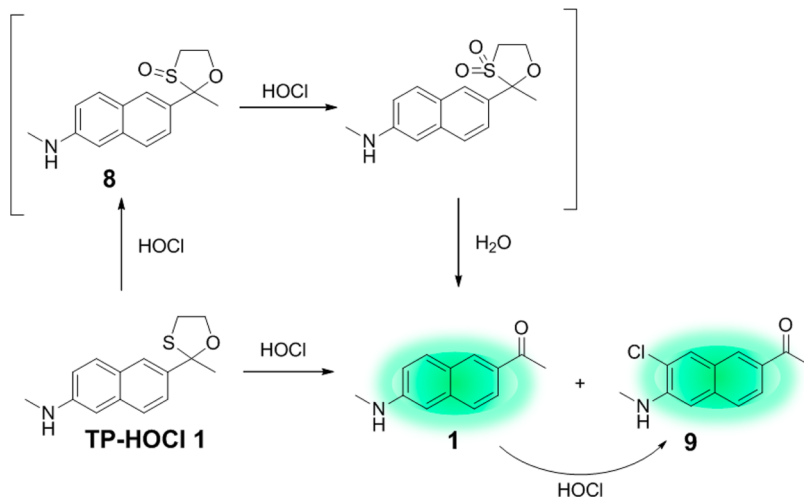


Figure 4. Proposed sensing mechanism of TP-HOCl 1 for HOCl.

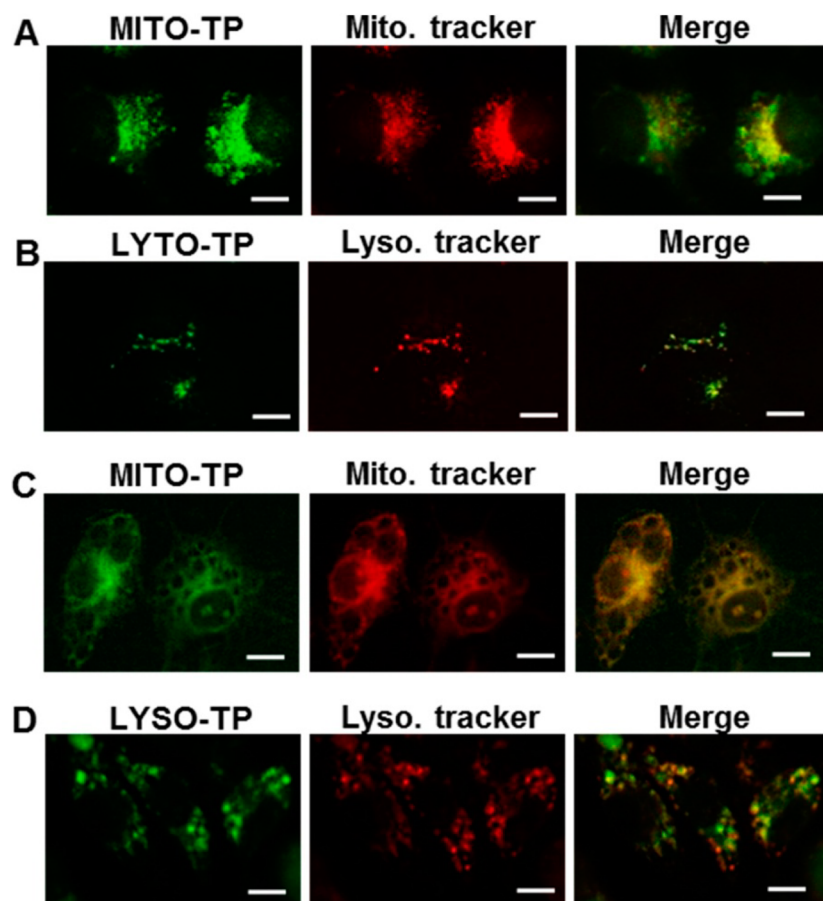


Figure 5. Intracellular localization of MITO-TP and LYSO-TP in HeLa (A, B) and macrophages cells (C, D). (A, B) Images of HeLa cells pretreated with 10 μ M MITO-TP (or 10 μ M LYSO-TP) for 20 min and subsequently 1 μ M Mito-Tracker Red (or 1 μ M Lyso-Tracker Red) for 10 min. Then cells were treated with 50 μ M HOCl for another 5 min. (C, D) Images of macrophage cells pretreated with LPS (120 ng/mL)/IFN- γ (20 ng/mL) for 24 h, then treated with 10 μ M MITO-TP (or 10 μ M LYSO-TP) for 20 min and subsequently 1 μ M Mito-Tracker Red (or 1 μ M Lyso-Tracker Red) for another 10 min. Green, probe fluorescence; red, Mito-Tracker and Lyso-Tracker fluorescence; yellow, merged signal. Scale bar: 10 μ m.

properties of compound 9, such as quantum yield and two-photon cross section, were measured, which suggests comparability with that of compound 1 (Table S2) thereby demonstrating little interference for further experiment. Taken together, a possible sensing mechanism of probe TP-HOCl 1 to HOCl is proposed and shown in Figure 4. Nonfluorescent TP-

HOCl 1 is initially oxidized by HOCl to intermediate sulfoxide compound 8, further oxidized to unstable Sulphone and finally hydrolyzed to generate fluorescent compound 1. Then compound 1 was partially chlorinated to compound 9 by excessive HOCl. In addition, to verify the above sensing mechanism, intermediate sulfoxide compound 8 was also

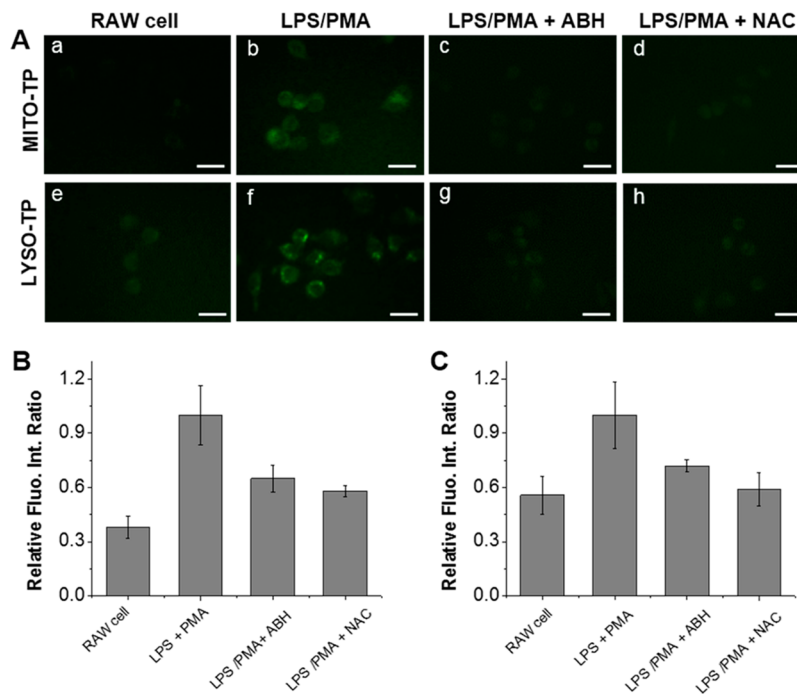


Figure 6. Detection of HOCl in live RAW 264.7 macrophage cells via MITO-TP and LYSO-TP. (A) Representative fluorescent images of macrophage cells. (a, e) MITO-TP or LYSO-TP ($15 \mu\text{M}$) was incubated with macrophages cells for 20 min and washed by PBS buffer. (b, f) Cells were preincubated with probes, washed by PBS buffer and stimulated with LPS ($1 \mu\text{g/mL}$)/PMA ($1 \mu\text{g/mL}$) for 1 h. (c, g) Cells were preincubated with probes, washed by PBS buffer and stimulated with LPS ($1 \mu\text{g/mL}$)/PMA ($1 \mu\text{g/mL}$) and ABH ($200 \mu\text{M}$) for 1 h. (d, h) Cells were preincubated with probes, washed by PBS buffer and stimulated with LPS ($1 \mu\text{g/mL}$)/PMA ($1 \mu\text{g/mL}$) and NAC (1mM) for 1 h. (B, C) Quantification of the fluorescence signals from (a)–(h). Data were normalized to the fluorescence intensity from LPS/PMA stimulated macrophage cells (b or f). Error bars are $\pm \text{SD}$, $n = 3$. Scale bar: $30 \mu\text{m}$.

prepared. Notably, compared with TP-HOCl 1, unstable compound 8 is more easily oxidized to compound 1 by HOCl (Figure S11), suggesting that sulfoxide compound 8 is the possible intermediate of the oxidation process.

Fluorescence Imaging of HOCl at the Subcellular Level. HOCl, as the key “killer” for pathogens during phagocytosis, is proposed to be mainly produced from MPO-catalyzed peroxidation of chloride ions in phagolysosomes. Recently, accumulating research demonstrates that non-phagosomal HOCl (nphHOCl) can also be produced after incubation with soluble stimuli.^{52,65} However, the organelles with intracellular nphHOCl are still unclear, which limits further elucidation of the corresponding functions of nphHOCl at subcellular level. Therefore, to clarify the distribution of HOCl at subcellular levels, mitochondria- (MITO-TP) and lysosome- (LYSO-TP) targetable derivatives of probe TP-HOCl 1 were synthesized through introducing triphenylphosphine⁶¹ or morpholine⁶⁰ to the amine group. Furthermore, in vitro experiment demonstrates that both MITO-TP and LYSO-TP can respond to HOCl at nanomolar level in PBS (1% DMSO, pH 7.4 and 5.0), respectively (Figure S12).

As shown in Figure S13, cell cytotoxicity of the probes was initially examined in HeLa cells, which proves that there is no significant cytotoxicity in the presence of $1\text{--}32 \mu\text{M}$ probe MITO-TP or LYSO-TP for 12 h. To determine the intracellular location of MITO-TP and LYSO-TP inside cells, the probe MITO-TP (or LYSO-TP) and Mito-Tracker Red (or Lyso-Tracker Red) were coincubated with live HeLa cells, which was treated HOCl ($50 \mu\text{M}$) for another 5 min. As expected, probe MITO-TP mainly localized in the mitochondria rather than lysosome and nucleus (Figures 5A and S14A), while LYSO-TP

mainly stained in the lysosome of live cells (Figures 5B and S14B). Meanwhile, the same subcellular distribution of MITO-TP and LYSO-TP can also be confirmed in LPS/IFN- γ -stimulated macrophage cells (Figures 5C, D and S15). After confirming the intracellular localization of LYSO-TP and MITO-TP, the distribution time of these probes were evaluated in RAW cells (shown in Figure S16). To efficiently track the probes in cells, compounds 4 and 7, the bright fluorescent precursors of LYSO-TP and MITO-TP, were used to examine the intracellular distribution time. As shown in Figure S16, the fluorescent intensity of compounds 4 and 7 rapidly reaches the equilibrium state within 20 min in RAW cells and keeps stable in at least 60 min. Based on the structural similarity of probes (LYSO-TP and MITO-TP) and their precursors (4 and 7), it is rational to assume that the probes LYSO-TP and MITO-TP can also quickly reach the equilibrium state inside cells and keep stable for some time.

After that, the detection of HOCl in mitochondria and lysosome was examined in murine live macrophage cell line RAW 264.7 (Figure 6). It was reported that targeting groups such as triphenylphosphine⁶⁶ and morpholine^{67,68} can significantly increase the distribution in mitochondria and lysosome respectively and relatively difficult to be washed out. Thus, RAW cells were incubated with MITO-TP and LYSO-TP for 20 min respectively and subsequently washed with PBS buffer to remove the free probes, which ensures that probes mainly localized in the targeted organelles (mitochondria and lysosome). As shown in Figure 6A (a, e), both MITO-TP and LYSO-TP stained cells showed very weak fluorescence. However, the intracellular fluorescence from both MITO-TP and LYSO-TP stained cells were much stronger when the cell

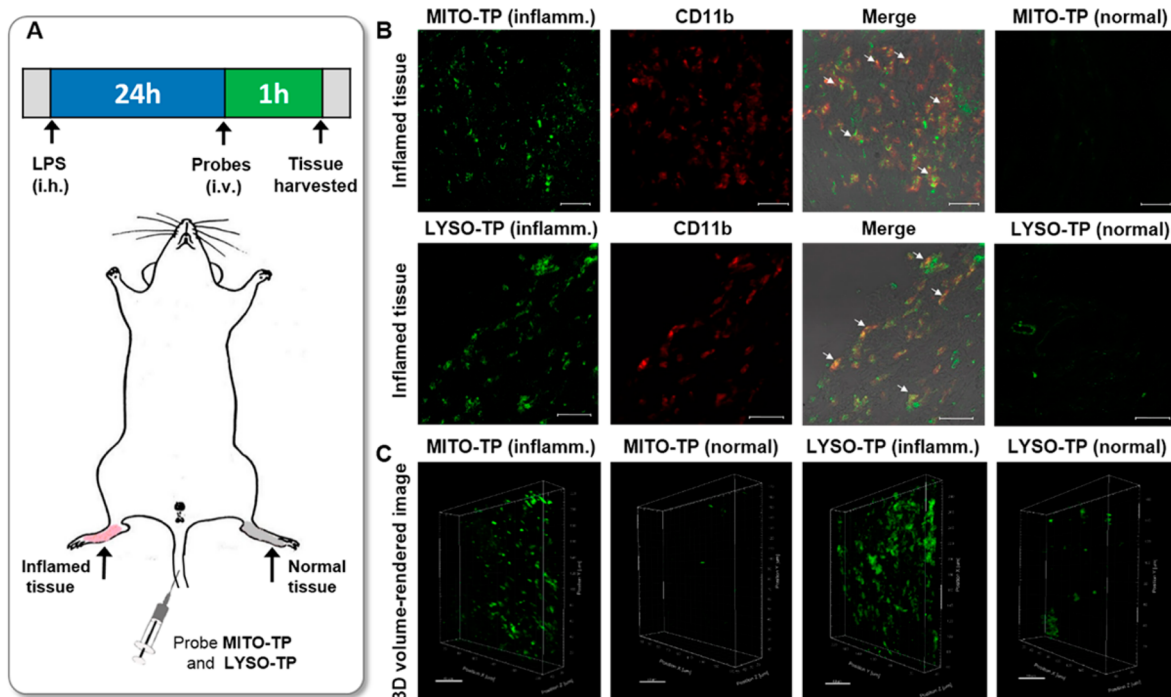


Figure 7. Detection of LPS-dependent HOCl generation in inflammation tissues via LYSO-TP and MITO-TP. (A) 200 μ L of LPS (1 mg/mL) was subcutaneously (i.h.) injected into right rear paws of mouse to cause inflammation. After 1 day, 200 μ L of 1 mM MITO-TP (or LYSO-TP) was intravenously (i.v.) injected and the paw skin was sectioned 1 h later. (B) Fluorescence images of probes and CD11b in the inflamed tissue. Probe fluorescence, green; antibody CD11b, red. Arrows indicate the merged parts of HOCl sensitive probes and CD11b. (C) 3D volume-rendered image shows the distribution of macrophages within the inflamed and normal tissues. (+) Inflammation tissues; (-) Normal tissues. Scale bar: 30 μ m.

was subsequently stimulated with lipopolysaccharides (LPS, 1 μ g/mL) and phorbol myristate acetate (PMA, 1 μ g/mL) together (Figure 6A (b, f) and B, C). Based on remarkable fluorescence increase from the probe localized organelles, it is evident that the increased fluorescence signal is mainly due to the reaction between probes and nonphagosomal HOCl in mitochondria and lysosome.⁶⁵ To further examine the above assumption, control experiments were performed, in which 4-aminobenzoic acid hydrazide (ABH) was added to decrease cellular HOCl level through inhibiting the activity of MPO.¹⁶ As shown in Figure 6A (c, g), cellular fluorescence intensity of both MITO-TP and LYSO-TP stained cells is suppressed to some extent when the stimulated RAW cells were incubated with 200 μ M ABH together. Similar phenomena were also observed in 24 h incubation of stimuli and ABH (Figure S17). In addition, the fluorescence of probes stained cells can also be reduced clearly by addition of *N*-acetylcysteine (NAC), a powerful ROS scavenger⁷¹ (Figure 6A (d, h) and B, C). This is mainly because most of the intracellular HOCl can be effectively removed by NAC, in which the thiol atom can react with HOCl rapidly. One possible reason for the existence of intracellular HOCl in both mitochondrial and lysosomal is the movement of intracellular HOCl between organelles. Another plausible reason is that nphHOCl could be in situ generated in both mitochondria and lysosome of LPS/PMA-stimulated macrophage cells. This is because the respiratory burst induced by LPS and PMA in mitochondria produces higher amount of H₂O₂,^{5,69,74} which can easily transfer to other organelles like the lysosome due to its good plasma membrane permeability.⁷⁰ Meanwhile, it is reported that MPO is located not only in lysosome but also in mitochondria of macrophage cells.^{50,51} Therefore, it is assumed that H₂O₂ may work with

MPO to produce nphHOCl in both mitochondria and lysosome.

Two-Photon Tissue Imaging of HOCl in Inflamed Mouse Model.

To examine whether nphHOCl can be *in vivo* detected in mitochondria and lysosome of macrophage cells in inflamed mouse model, 200 μ L of LPS (1 mg/mL) was subcutaneously injected into right rear paws of mice to cause inflammation (Figure 7A). After 1 day, MITO-TP and LYSO-TP were intravenously injected and the paw skin was sectioned 1 h later. As shown in Figure 7B, strong fluorescence from both MITO-TP and LYSO-TP in LPS-stimulated macrophage cells was observed in inflammation tissues (shown in green color), which was further confirmed by immunostaining of histological sections with macrophage marker CD11b (shown in red color). However, the signals from both probes and macrophage marker remained largely negative in the normal tissues (Figures 7B and S18).

Besides, the fluorescence from MITO-TP and LYSO-TP was collected at different depths in inflamed tissues and reconstructed in a three-dimensional (3D) box to describe the spatial distribution of LPS-stimulated macrophage cells (Figure 7C). Taken together, MITO-TP and LYSO-TP were successfully applied to stain the macrophage cells in inflamed mouse model through intravenous injection. Importantly, it is indicated that much higher concentration of nphHOCl in both mitochondria and lysosome of macrophage cells could be detected during inflammation.

CONCLUSION

In summary, we have developed the first two-photon fluorescent “turn-on” HOCl probe (TP-HOCl 1) and its mitochondria (MITO-TP) and lysosome (LYSO-TP) target-

able derivatives to image HOCl among corresponding organelles. Because of the unique oxidation deprotection mechanism, these probes show not only fast response (within seconds) and good sensitivity (<20 nM) to HOCl but also high selectivity over other ROS and biomolecules. Cell imaging experiments indicate that probes Mito-TP and LYSO-TP display good cell penetration and localize in mitochondria and lysosome of living cells, respectively. Furthermore, it was indicated that HOCl may be detected in both mitochondria and lysosome of LPS/PMA-stimulated macrophage cells. In particular, two-photon imaging shows that a much larger amount of HOCl can be detected in both lysosome and mitochondria of macrophage cells during inflammation conditions in a murine model. Therefore, due to the advantages of these probes, they not only can help elucidate the distribution of subcellular HOCl, but also serve as excellent tools to exploit potential functions of HOCl at subcellular and tissue levels.

■ ASSOCIATED CONTENT

Supporting Information

Synthesis, additional spectroscopic and imaging data, Gaussian calculation results, and MTT results. The Supporting Information is available free of charge on the ACS Publications website at DOI: 10.1021/jacs.5b00042.

■ AUTHOR INFORMATION

Corresponding Author

*chmcyt@nus.edu.sg

Author Contributions

[†]L.Y. and L.W. contributed equally.

Notes

The authors declare no competing financial interest.

■ ACKNOWLEDGMENTS

This work was supported by intramural funding from A*STAR (Agency for Science, Technology and Research, Singapore) Biomedical Research Council and National Medical Research Council grant (NMRC/CBRG/0015/2012).

■ REFERENCES

- (1) Finkel, T.; Holbrook, N. J. *Nature* **2000**, *408*, 239.
- (2) Branzk, N.; Lubojemska, A.; Hardison, S. E.; Wang, Q.; Gutierrez, M. G.; Brown, G. D.; Papayannopoulos, V. *Nat. Immunol.* **2014**, *15*, 1017.
- (3) Strowig, T.; Henao-Mejia, J.; Elinav, E.; Flavell, R. *Nature* **2012**, *481*, 278.
- (4) Winterbourn, C. C.; Hampton, M. B.; Livesey, J. H.; Kettle, A. J. *J. Biol. Chem.* **2006**, *281*, 39860.
- (5) Klebanoff, S. J. *J. Leukocyte Biol.* **2005**, *77*, 598.
- (6) Koide, Y.; Urano, Y.; Hanaoka, K.; Terai, T.; Nagano, T. *J. Am. Chem. Soc.* **2011**, *133*, 5680.
- (7) Kobayashi, T.; Robinson, J. M.; Seguchi, H. *J. Cell Sci.* **1998**, *111* (Pt 1), 81.
- (8) Whiteman, M.; Rose, P.; Siau, J. L.; Cheung, N. S.; Tan, G. S.; Halliwell, B.; Armstrong, J. S. *Free Radical Biol. Med.* **2005**, *38*, 1571.
- (9) Matute, J. D.; Arias, A. A.; Wright, N. A.; Wrobel, I.; Waterhouse, C. C.; Li, X. J.; Marchal, C. C.; Stull, N. D.; Lewis, D. B.; Steele, M.; Kellner, J. D.; Yu, W.; Meroueh, S. O.; Nauseef, W. M.; Dinauer, M. C. *Blood* **2009**, *114*, 3309.
- (10) Yap, Y. W.; Whiteman, M.; Cheung, N. S. *Cell Signalling* **2007**, *19*, 219.
- (11) Choi, D. K.; Pennathur, S.; Perier, C.; Tieu, K.; Teismann, P.; Wu, D. C.; Jackson-Lewis, V.; Vila, M.; Vonsattel, J. P.; Heinecke, J. W.; Przedborski, S. *J. Neurosci.* **2005**, *25*, 6594.
- (12) Miljkovic-Lolic, M.; Silbergleit, R.; Fiskum, G.; Rosenthal, R. E. *Brain Res.* **2003**, *971*, 90.
- (13) Yang, Y. T.; Whiteman, M.; Gieseg, S. P. *Biochim. Biophys. Acta* **2012**, *1823*, 420.
- (14) Yap, Y. W.; Whiteman, M.; Bay, B. H.; Li, Y.; Sheu, F. S.; Qi, R. Z.; Tan, C. H.; Cheung, N. S. *J. Neurochem.* **2006**, *98*, 1597.
- (15) Bylund, J.; Brown, K. L.; Movitz, C.; Dahlgren, C.; Karlsson, A. *Free Radical Biol. Med.* **2010**, *49*, 1834.
- (16) Klebanoff, S. J.; Kettle, A. J.; Rosen, H.; Winterbourn, C. C.; Nauseef, W. M. *J. Leukoc. Biol.* **2013**, *93*, 185.
- (17) Winterbourn, C. C. *Toxicology* **2002**, *181*, 223.
- (18) Aratani, Y.; Koyama, H.; Nyui, S.; Suzuki, K.; Kura, F.; Maeda, N. *Infect. Immun.* **1999**, *67*, 1828.
- (19) J Cell Sci/Fernandez-Suarez, M.; Ting, A. Y. *Nat. Rev. Mol. Cell. Biol.* **2008**, *9*, 929.
- (20) Chan, J.; Dodani, S. C.; Chang, C. J. *Nat. Chem.* **2012**, *4*, 973.
- (21) Dickinson, B. C.; Chang, C. J. *J. Am. Chem. Soc.* **2008**, *130*, 9638.
- (22) Lim, S. Y.; Hong, K. H.; Kim, D. I.; Kwon, H.; Kim, H. J. *J. Am. Chem. Soc.* **2014**, *136*, 7018.
- (23) Lee, M. H.; Park, N.; Yi, C.; Han, J. H.; Hong, J. H.; Kim, K. P.; Kang, D. H.; Sessler, J. L.; Kang, C.; Kim, J. S. *J. Am. Chem. Soc.* **2014**, *136*, 14136.
- (24) Ishida, M.; Watanabe, H.; Takigawa, K.; Kurishita, Y.; Oki, C.; Nakamura, A.; Hamachi, I.; Tsukiji, S. *J. Am. Chem. Soc.* **2013**, *135*, 12684.
- (25) Arai, S.; Lee, S.-C.; Zhai, D.; Suzuki, M.; Chang, Y. T. *Sci. Rep.* **2014**, *4*, 6701.
- (26) Kim, H. M.; Cho, B. R. *Acc. Chem. Res.* **2009**, *42*, 863.
- (27) Helmchen, F.; Denk, W. *Nat. Methods* **2005**, *2*, 932.
- (28) Kim, D.; Ryu, H. G.; Ahn, K. H. *Org. Biomol. Chem.* **2014**, *12*, 4550.
- (29) Yuan, L.; Jin, F.; Zeng, Z.; Liu, C.; Luo, S.; Wu, J. *Chem. Sci.* **2015**, *6*, 2360–2365.
- (30) Chen, X.; Wang, X.; Wang, S.; Shi, W.; Wang, K.; Ma, H. *Chem.—Eur. J.* **2008**, *14*, 4719.
- (31) Sun, Z. N.; Liu, F. Q.; Chen, Y.; Tam, P. K.; Yang, D. *Org. Lett.* **2008**, *10*, 2171.
- (32) Hu, J. J.; Wong, N. K.; Gu, Q.; Bai, X.; Ye, S.; Yang, D. *Org. Lett.* **2014**, *16*, 3544.
- (33) Lin, W.; Long, L.; Chen, B.; Tan, W. *Chem.—Eur. J.* **2009**, *15*, 2305.
- (34) Cheng, X.; Jia, H.; Long, T.; Feng, J.; Qin, J.; Li, Z. *Chem. Commun.* **2011**, *47*, 11978.
- (35) Emrullahoglu, M.; Ucuncu, M.; Karakus, E. *Chem. Commun.* **2013**, *49*, 7836.
- (36) Zhao, N.; Wu, Y. H.; Wang, R. M.; Shi, L. X.; Chen, Z. N. *Analyst* **2011**, *136*, 2277.
- (37) Cheng, G.; Fan, J.; Sun, W.; Cao, J.; Hu, C.; Peng, X. *Chem. Commun.* **2014**, *50*, 1018.
- (38) Liu, S. R.; Wu, S. P. *Org. Lett.* **2013**, *15*, 878.
- (39) Li, G.; Zhu, D.; Liu, Q.; Xue, L.; Jiang, H. *Org. Lett.* **2013**, *15*, 2002.
- (40) Qu, Z.; Ding, J.; Zhao, M.; Li, P. *J. Photochem. Photobiol. A* **2015**, *299*, 1.
- (41) Zhan, X.-Q.; Yan, J.-H.; Su, J.-H.; Wang, Y.-C.; He, J.; Wang, S.-Y.; Zheng, H.; Xu, J.-G. *Sens. Actuators, B* **2010**, *150*, 774.
- (42) Chen, X.; Lee, K. A.; Ha, E. M.; Lee, K. M.; Seo, Y. Y.; Choi, H. K.; Kim, H. N.; Kim, M. J.; Cho, C. S.; Lee, S. Y.; Lee, W. J.; Yoon, J. *Chem. Commun.* **2011**, *47*, 4373.
- (43) Xu, Q.; Lee, K. A.; Lee, S.; Lee, K. M.; Lee, W. J.; Yoon, J. *J. Am. Chem. Soc.* **2013**, *135*, 9944.
- (44) Wu, X. J.; Li, Z.; Yang, L.; Han, J. H.; Han, S. F. *Chem. Sci.* **2013**, *4*, 460.
- (45) Zhang, R.; Ye, Z.; Song, B.; Dai, Z.; An, X.; Yuan, J. *Inorg. Chem.* **2013**, *52*, 10325.

- (46) Xiao, H.; Xin, K.; Dou, H.; Yin, G.; Quan, Y.; Wang, R. *Chem. Commun.* **2015**, *51*, 1442.
- (47) Ye, Z.; Zhang, R.; Song, B.; Dai, Z.; Jin, D.; Goldys, E. M.; Yuan, J. *Dalton Trans.* **2014**, *43*, 8414.
- (48) Yuan, L.; Lin, W.; Xie, Y.; Chen, B.; Song, J. *Chem.—Eur. J.* **2012**, *18*, 2700.
- (49) Zhu, H.; Fan, J.; Wang, J.; Mu, H.; Peng, X. *J. Am. Chem. Soc.* **2014**, *136*, 12820.
- (50) Nauseef, W. M. *Blood* **1987**, *70*, 1143.
- (51) de Araujo, T. H.; Okada, S. S.; Ghosn, E. E.; Taniwaki, N. N.; Rodrigues, M. R.; de Almeida, S. R.; Mortara, R. A.; Russo, M.; Campa, A.; Albuquerque, R. C. *Cell Immunol.* **2013**, *281*, 27.
- (52) Li, G.; Lin, Q.; Ji, L.; Chao, H. *J. Mater. Chem. B* **2014**, *2*, 7918.
- (53) Wu, X.; Li, Z.; Yang, L.; Han, J.; Han, S. *Chem. Sci.* **2013**, *4*, 460.
- (54) Kim, H. M.; Seo, M. S.; An, M. J.; Hong, J. H.; Tian, Y. S.; Choi, J. H.; Kwon, O.; Lee, K. J.; Cho, B. R. *Angew. Chem., Int. Ed.* **2008**, *47*, 5167.
- (55) Rao, A. S.; Kim, D.; Nam, H.; Jo, H.; Kim, K. H.; Ban, C.; Ahn, K. H. *Chem. Commun.* **2012**, *48*, 3206.
- (56) Rao, A. S.; Kim, D.; Wang, T.; Kim, K. H.; Hwang, S.; Ahn, K. H. *Org. Lett.* **2012**, *14*, 2598.
- (57) Kim, H. M.; An, M. J.; Hong, J. H.; Jeong, B. H.; Kwon, O.; Hyon, J. Y.; Hong, S. C.; Lee, K. J.; Cho, B. R. *Angew. Chem., Int. Ed.* **2008**, *47*, 2231.
- (58) Hawkins, C. L.; Pattison, D. I.; Davies, M. J. *Amino Acids* **2003**, *25*, 259.
- (59) Reja, S. I.; Bhalla, V.; Sharma, A.; Kaur, G.; Kumar, M. *Chem. Commun.* **2014**, *50*, 11911.
- (60) Yu, H.; Xiao, Y.; Jin, L. *J. Am. Chem. Soc.* **2012**, *134*, 17486.
- (61) Lee, M. H.; Han, J. H.; Lee, J. H.; Choi, H. G.; Kang, C.; Kim, J. S. *J. Am. Chem. Soc.* **2012**, *134*, 17314.
- (62) Oakes, J.; Gratton, P. *J. Chem. Soc., Perkin Trans. 2* **1998**, 2201.
- (63) Xiao, H.; Xin, K.; Dou, H.; Yin, G.; Quan, Y.; Wang, R. *Chem. Commun.* **2015**, *51*, 1442.
- (64) Zhang, Y. R.; Chen, X. P.; Jing, S.; Zhang, J. Y.; Yuan, Q.; Miao, J. Y.; Zhao, B. X. *Chem. Commun.* **2014**, *50*, 14241.
- (65) Muijsers, R. B.; van Den Worm, E.; Folkerts, G.; Beukelman, C. J.; Koster, A. S.; Postma, D. S.; Nijkamp, F. P. *Br. J. Pharmacol.* **2000**, *130*, 932.
- (66) Murphy, M. P.; Smith, R. A. *Annu. Rev. Pharmacol. Toxicol.* **2007**, *47*, 629.
- (67) de Duve, C.; de Barsy, T.; Poole, B.; Trouet, A.; Tulkens, P.; Van Hoof, F. *Biochem. Pharmacol.* **1974**, *23*, 2495.
- (68) Firestone, R. A.; Pisano, J. M.; Bonney, R. J. *J. Med. Chem.* **1979**, *22*, 1130.
- (69) Schroder, K.; Hertzog, P. J.; Ravasi, T.; Hume, D. A. *J. Leukocyte Biol.* **2004**, *75*, 163.
- (70) Henzler, T.; Steudle, E. *J. Exp. Bot.* **2000**, *51*, 2053.
- (71) Witko-Sarsat, V.; Gausson, V.; Nguyen, A. T.; Touam, M.; Drueke, T.; Santangelo, F.; Descamps-Latscha, B. *Kidney Int.* **2003**, *64*, 82.
- (72) Kenmoku, S.; Urano, Y.; Kojima, H.; Nagano, T. *J. Am. Chem. Soc.* **2007**, *129*, 7313.
- (73) Hou, J.-T.; Wu, M.-Y.; Li, K.; Yang, J.; Yu, K.-K.; Xie, Y.-M.; Yu, X.-Q. *Chem. Commun.* **2014**, *50*, 8640.
- (74) Michaelis, J.; Vissers, M. C.; Winterbourn, C. C. *Arch. Biochem. Biophys.* **1992**, *2*, 555.